Matter, Volume *2*

Supplemental Information

Single-Molecule Toroic Design through Magnetic Exchange Coupling

Hao-Lan Zhang, Yuan-Qi Zhai, Lei Qin, Liviu Ungur, Hiroyuki Nojiri, and Yan-Zhen Zheng

Supplemental Information

I. Supplemental Figures

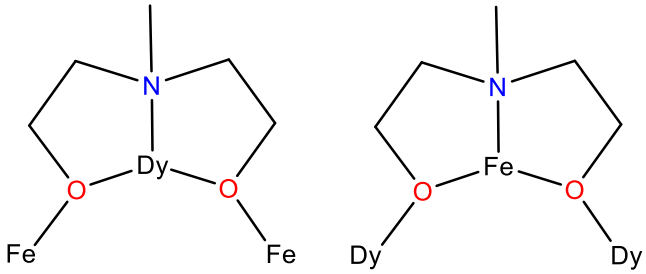

3.212 3.212

Figure S1. The two kinds of 3.212 (Harris notation) coordination modes of $mdea^{2-}$ in compounds **1Dy**. Harris notation describes the binding mode as $[X.Y_1Y_2Y_3. . .Y_n]$, where X is the overall number of metals bound by the whole ligand, and each value of Y refers to the number of metal atoms attached to the different donor atoms. See Coxall, R. A. *et al*. *J. Chem. Soc., Dalton Trans.* 2349–2356 (2000).

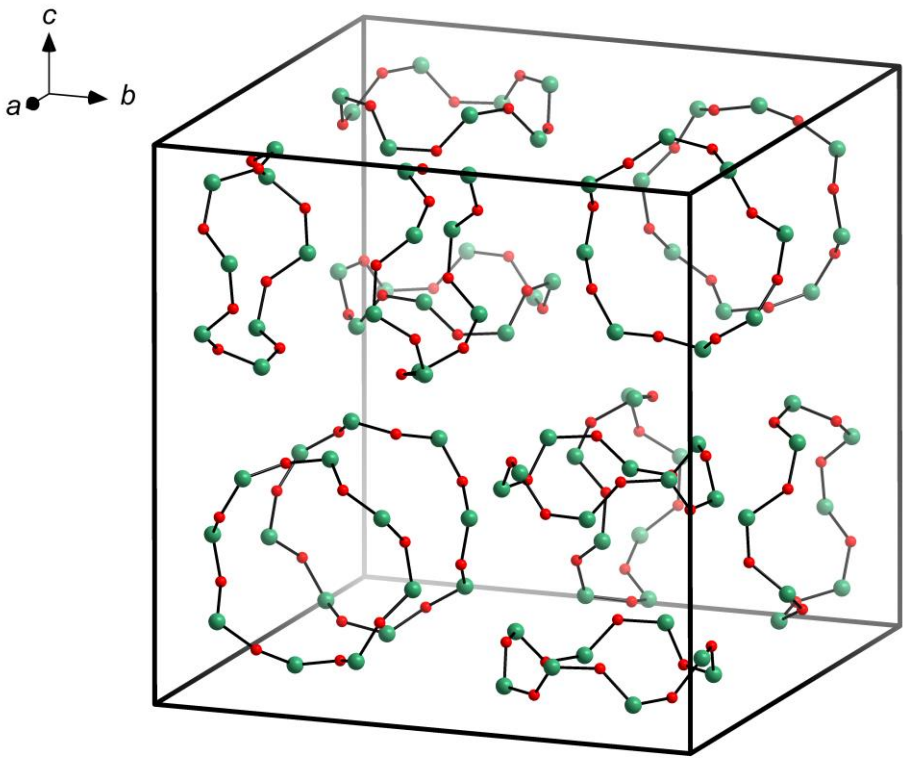

Figure S2. Molecular packing in unit cell of **1Dy**. Color codes: Fe, red; Dy, sea green. The non-metallic atoms were omitted for clarity.

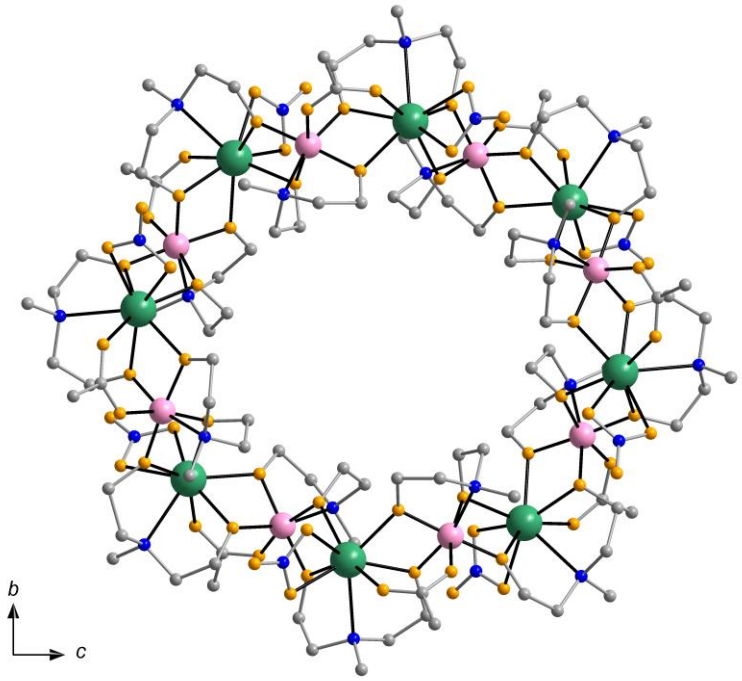

Figure S3. The molecular structure of complex **2Dy**. Color codes: Al, rose; Dy, sea green; C, grey; N, blue; O, light orange. The solvent molecules and hydrogen atoms were omitted for clarity. The Dy−O distances are ranging from 2.28 to 2.48 Å. The Dy−N (from $mdea^{2-}$) distances are in the range of 2.57 - 2.88 Å.

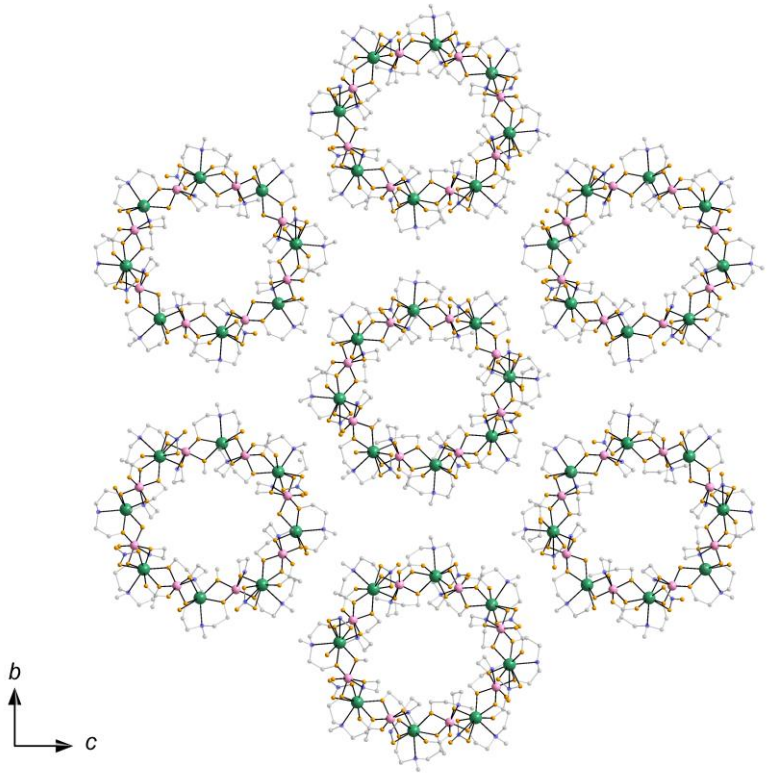

Figure S4. Molecular packing of complex **2Dy**. Color codes: Al, rose; Dy, sea green; C, grey; N, blue; O, light orange. The hydrogen atoms were omitted for clarity.

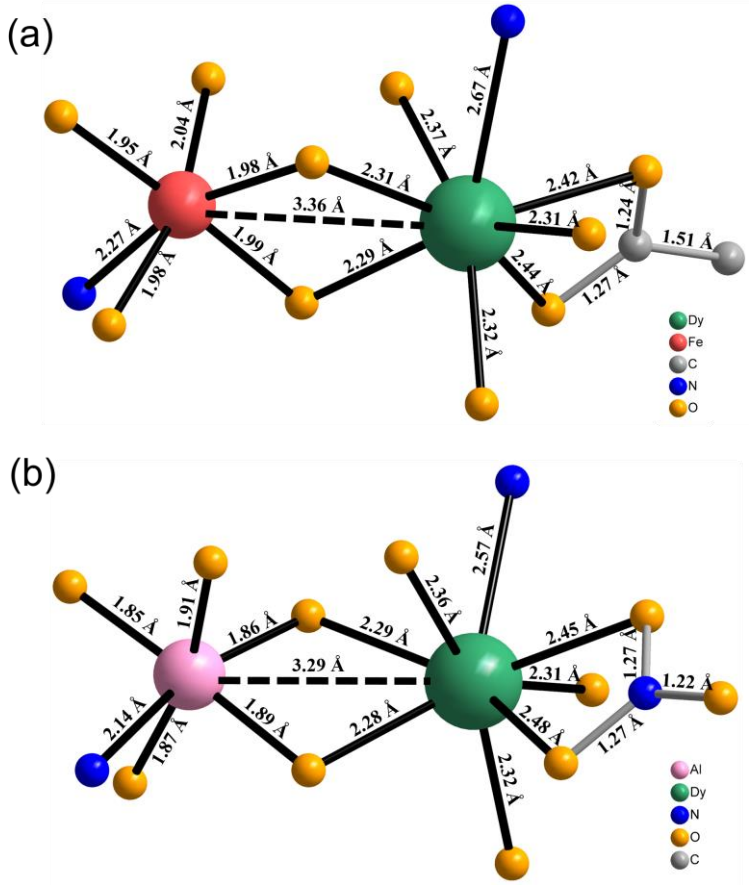

Figure S5. Local coordination environment of complexes **1Dy** (a) and **2Dy** (b).

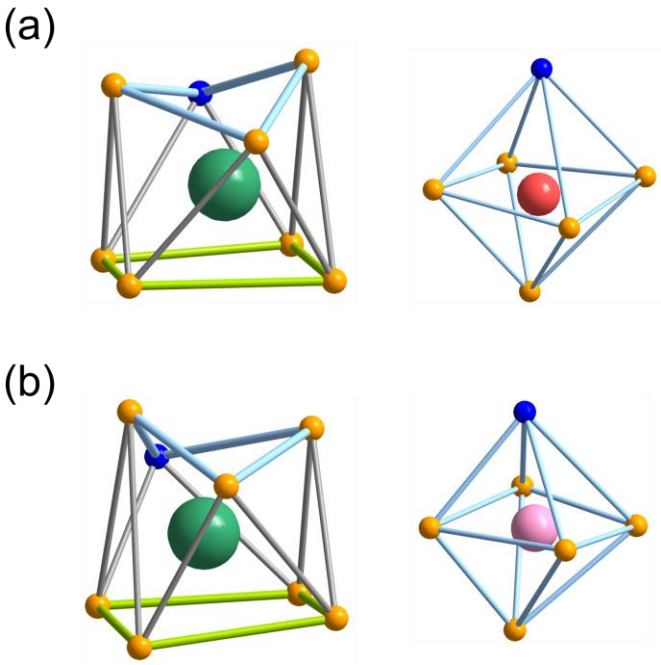

Figure S6. Coordination mode on metal centers of **1Dy** (a) and **2Dy** (b). Fe, red; Al, rose; Dy, sea green; N, blue; O, light orange.

(a)

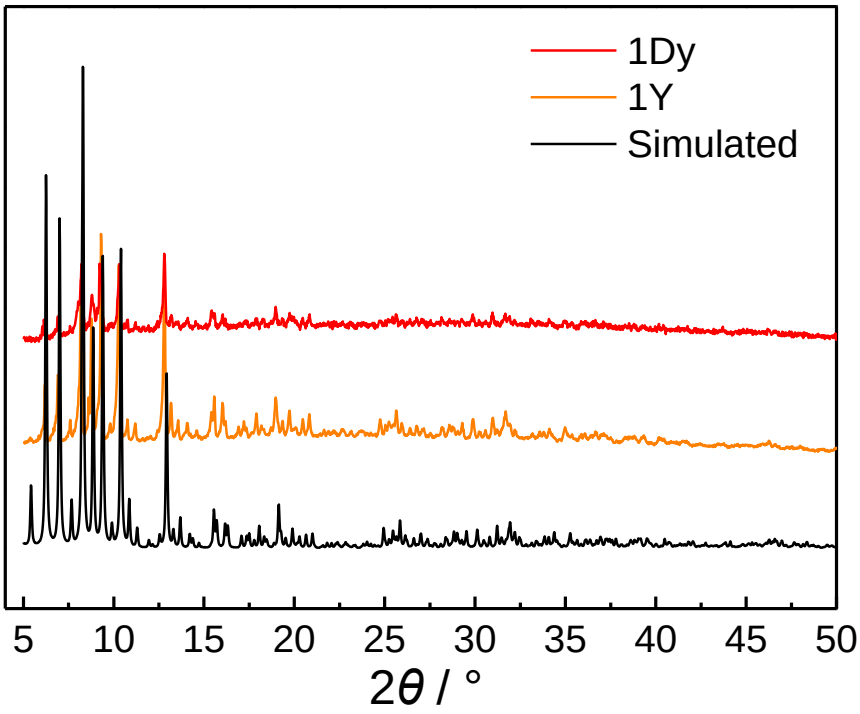

(b)

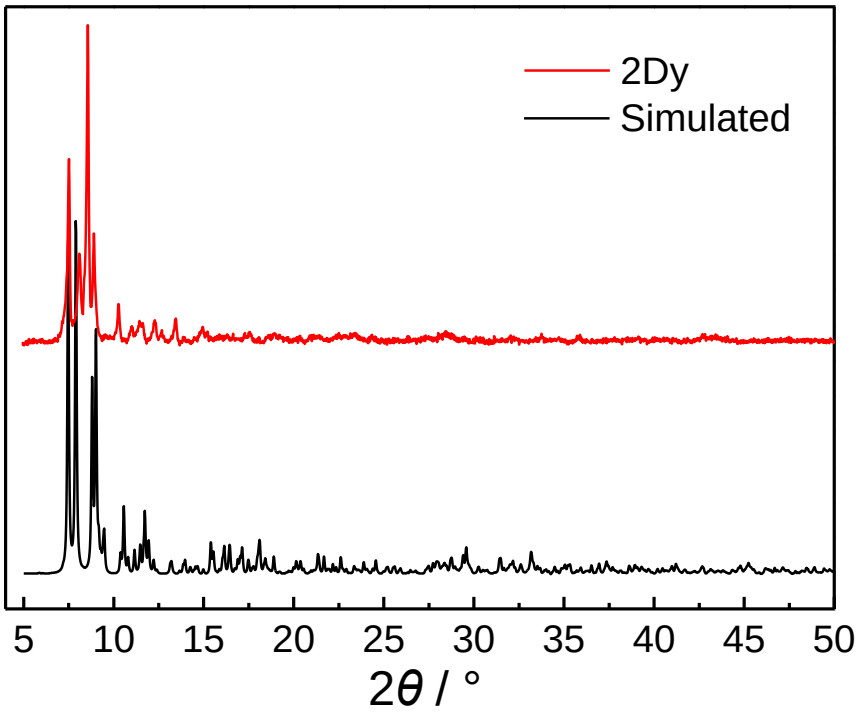

Figure S7. PXRD spectra for **1Dy** and **1Y** (a) and **2Dy** (b).

(a)

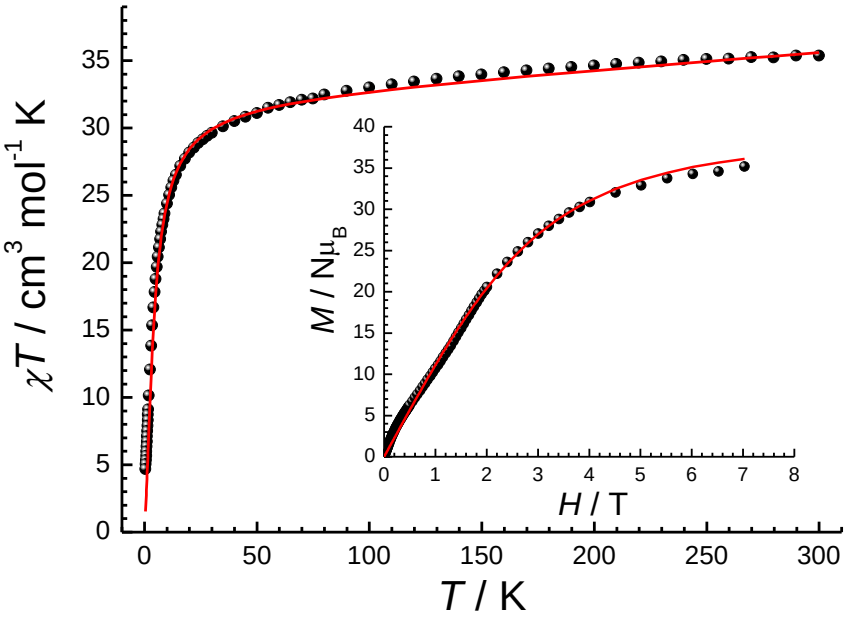

(b)

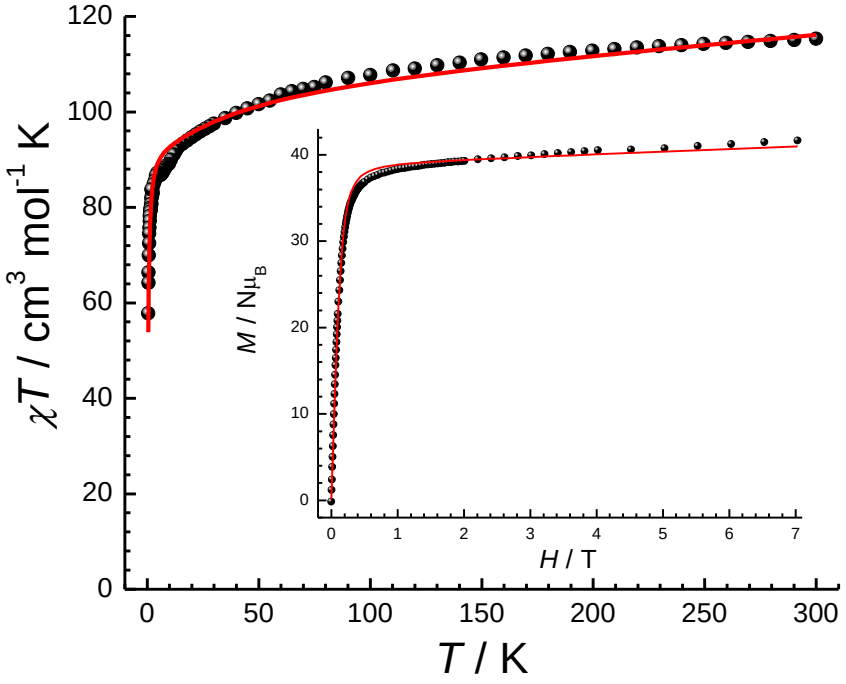

Figure S8. Temperature-dependent dc magnetic susceptibility plots of **1Y** from 0.5 to 300 K under 1000 Oe dc field. The red solid lines are BS-DFT fits of the data. Inset: Field-dependent magnetization plots at 0.5 K (a); Temperature-dependent dc magnetic susceptibility plots of **2Dy** from 0.5 to 300 K under 1000 Oe dc field. The red solid lines are POLY_ANISO fits of the data. Inset: Field-dependent magnetization plots at 0.5 K (b) .

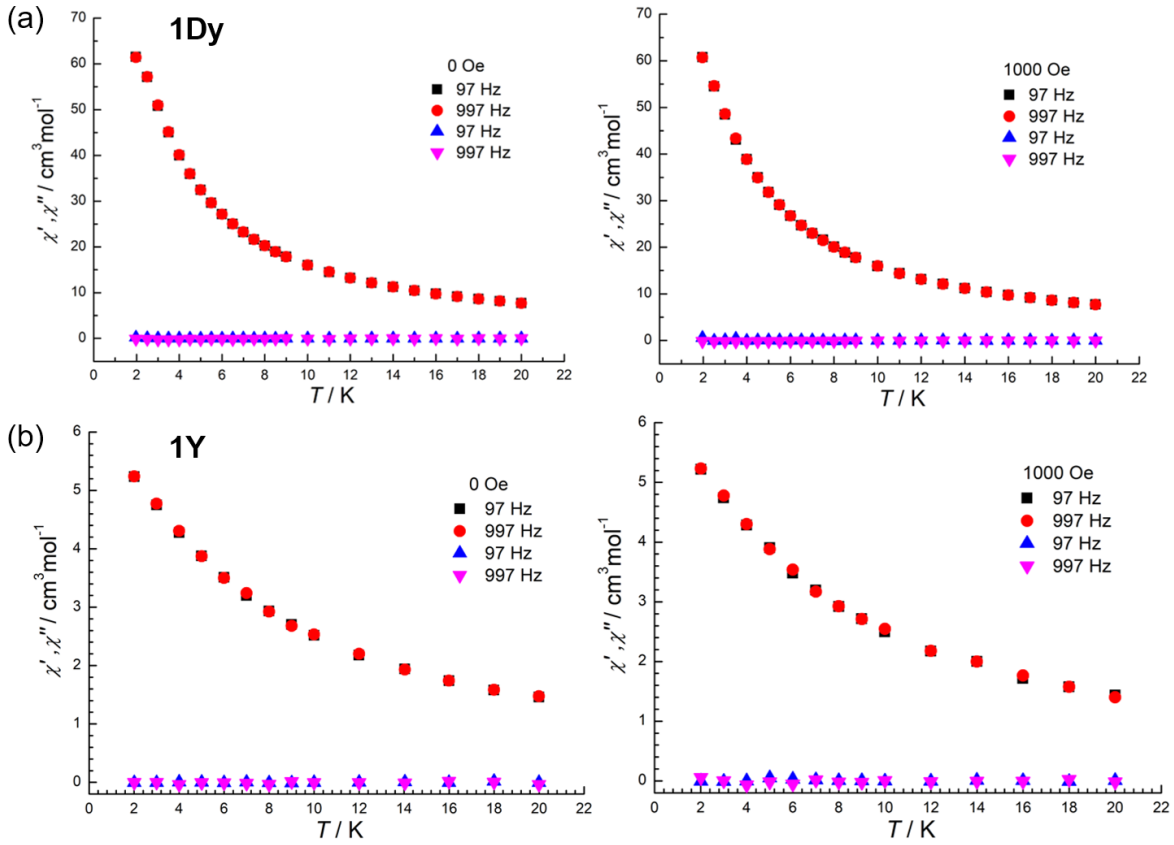

Figure S9. Temperature dependence of the ac susceptibilities for **1Dy** (a) and **1Y** (b) at the indicated frequencies under 0 Oe and 1000 Oe dc fields.

(a)

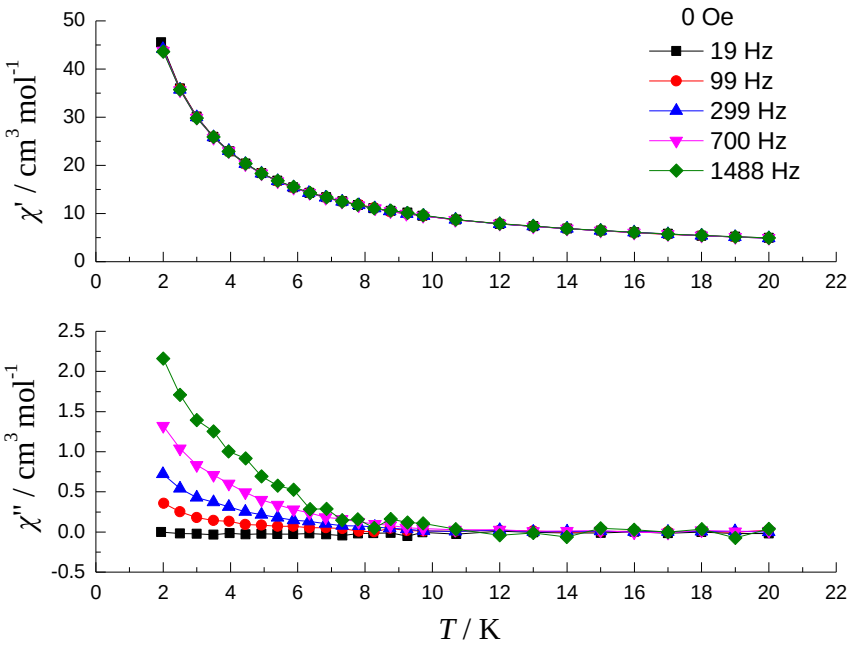

(b)

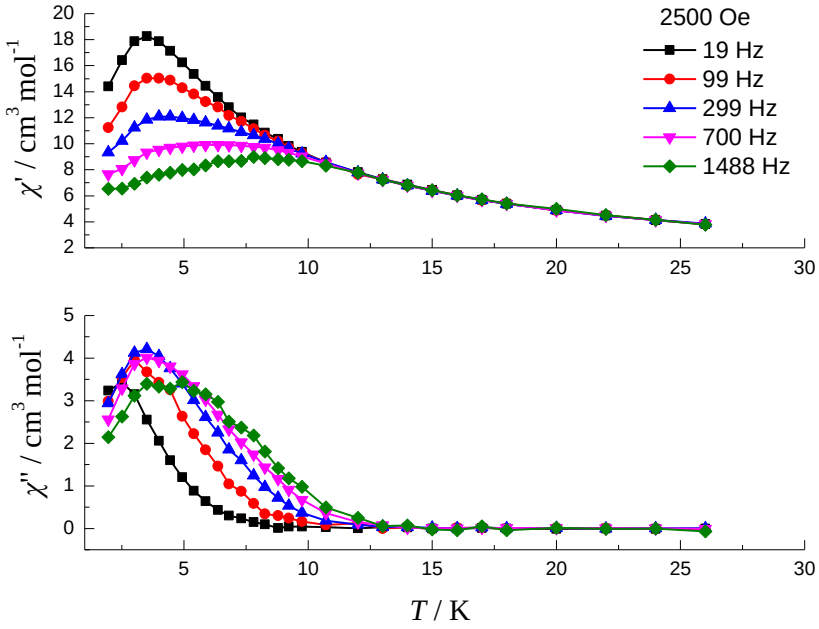

Figure S10. Ac magnetic susceptibility signals for **2Dy** under 0 Oe (a) and 2500 Oe (b) dc field at the indicated frequencies.

(a)

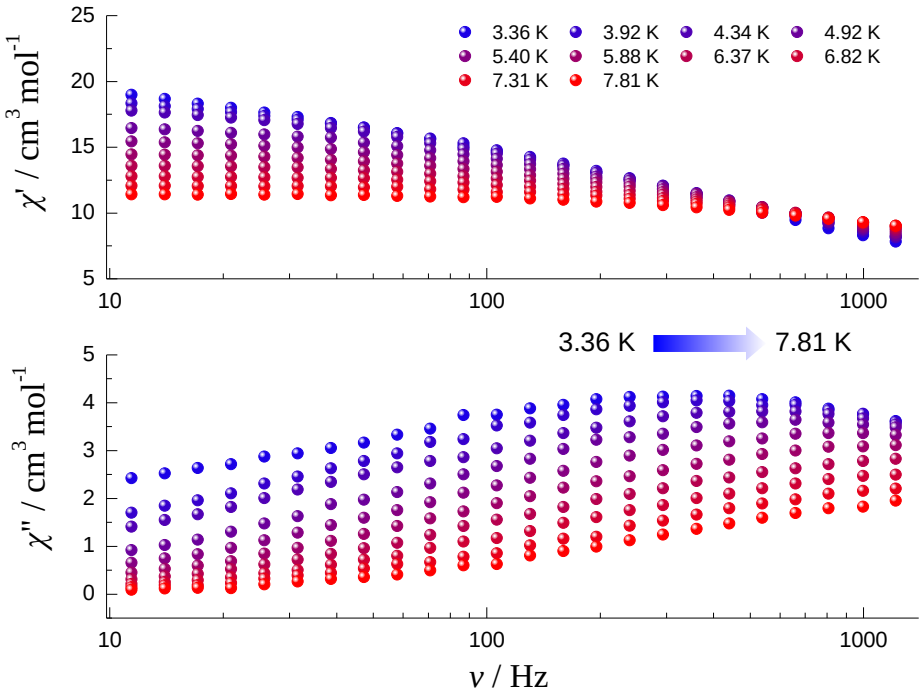

(b)

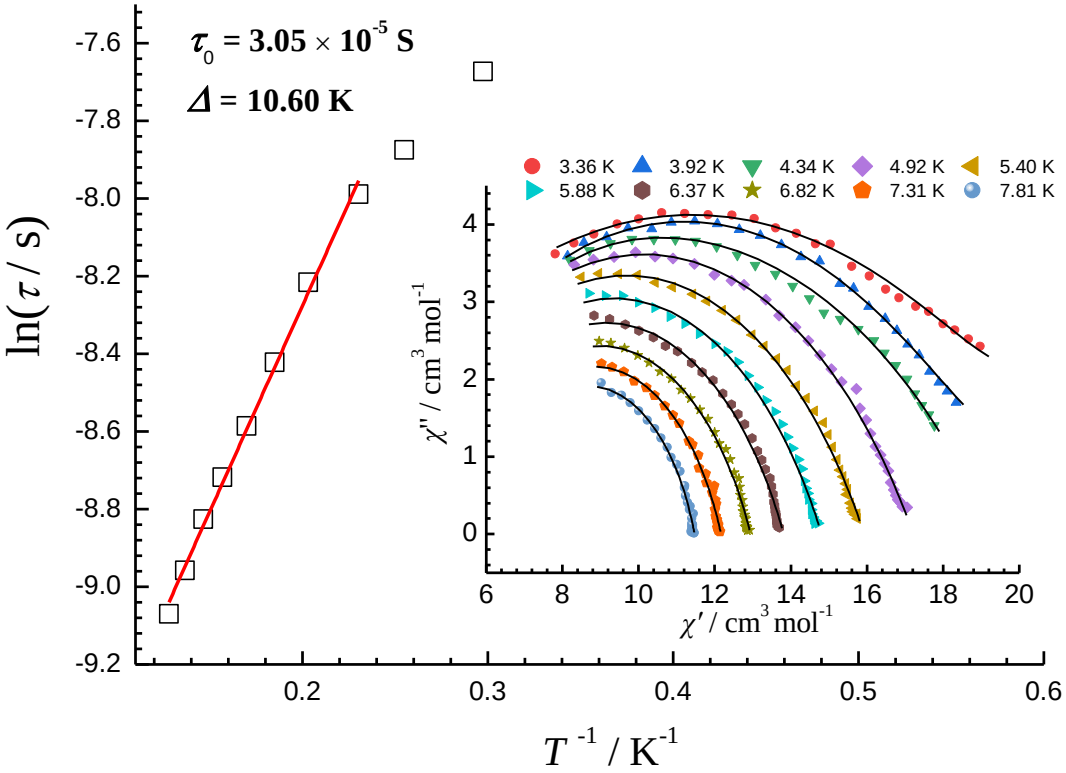

Figure S11. Variable-frequency ac magnetic susceptibility signals for **2Dy** under 2500 Oe dc field from 3.36 to 7.81 K (a); Plots of ln(τ) versus 1/T for **2Dy** and the linear fitting (b); Inset: Cole–Cole plots for **2Dy** obtained under 2500 Oe dc field.

(a)

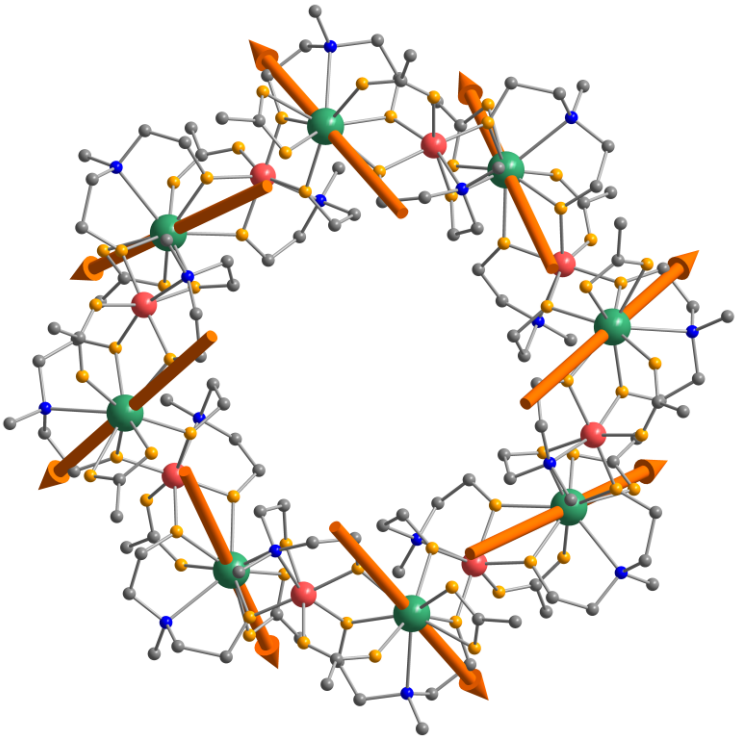

(b)

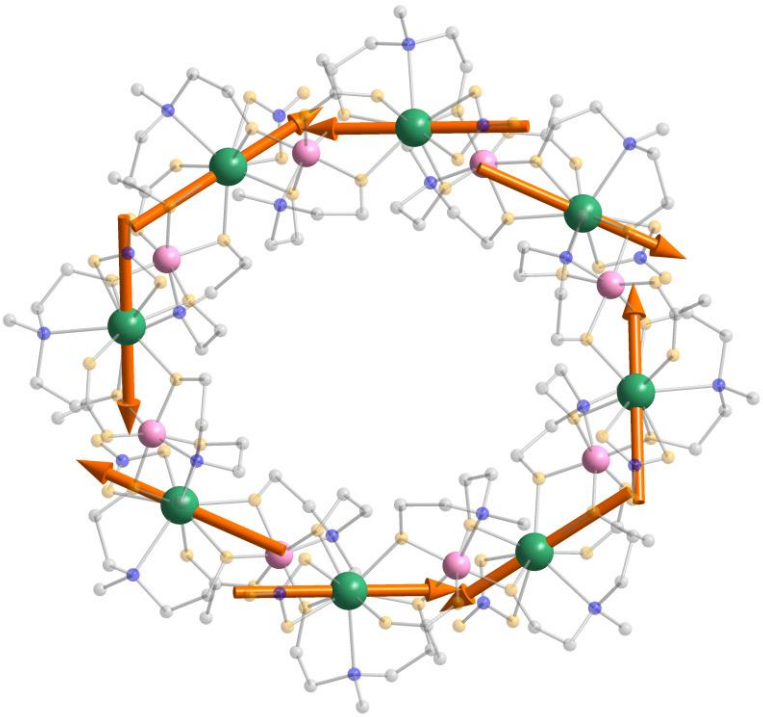

Figure S12. The ground state anisotropy directions (orange arrows) for the Dy^{III} ions in **1Dy** (a) and **2Dy** (b).

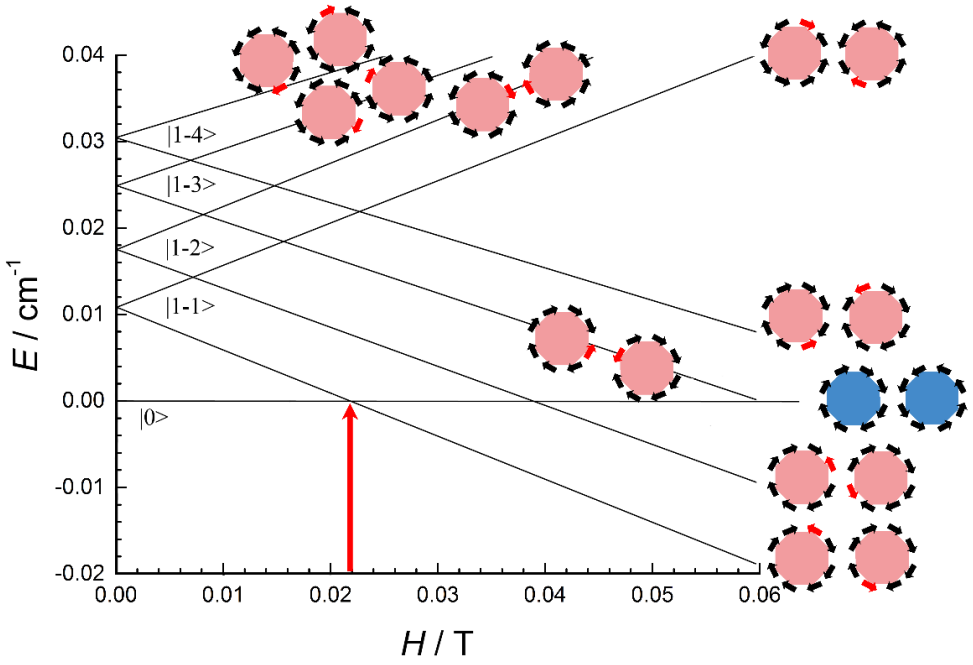

Figure S13. Energy levels for **2Dy** as function of magnetic field (Zeeman spectrum). Schematic non-collinear magnetic structure of the ground state (blue) and the first excited state (pink) of **2Dy**. Red vertical arrow represents the level crossing point at 0.022 T. The short arrows surrounding the circle are the local magnetic moments of Dy^{III} in the ground exchange doublet, in which red arrows represent the reversal of magnetization directions while the black ones represent original magnetization directions.

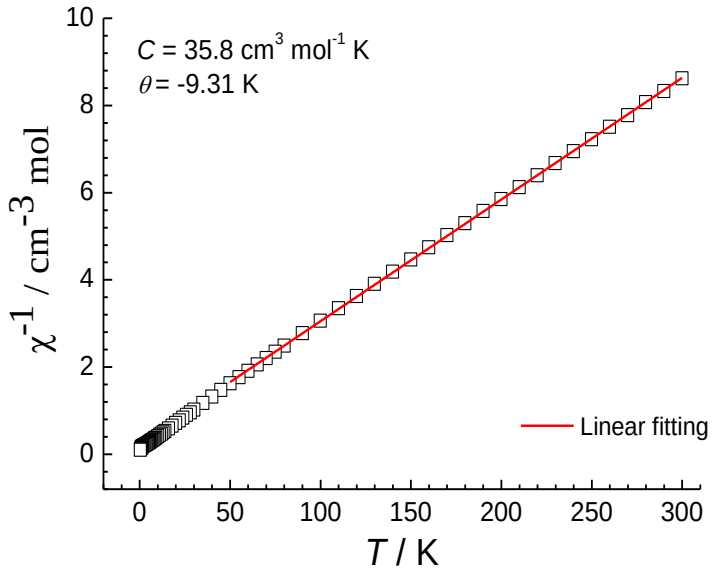

Figure S14. The Curie-Weiss fittings of the χ^{-1} vs. T plot under 1000 Oe dc field from 50 to 300 K for **1Y.**

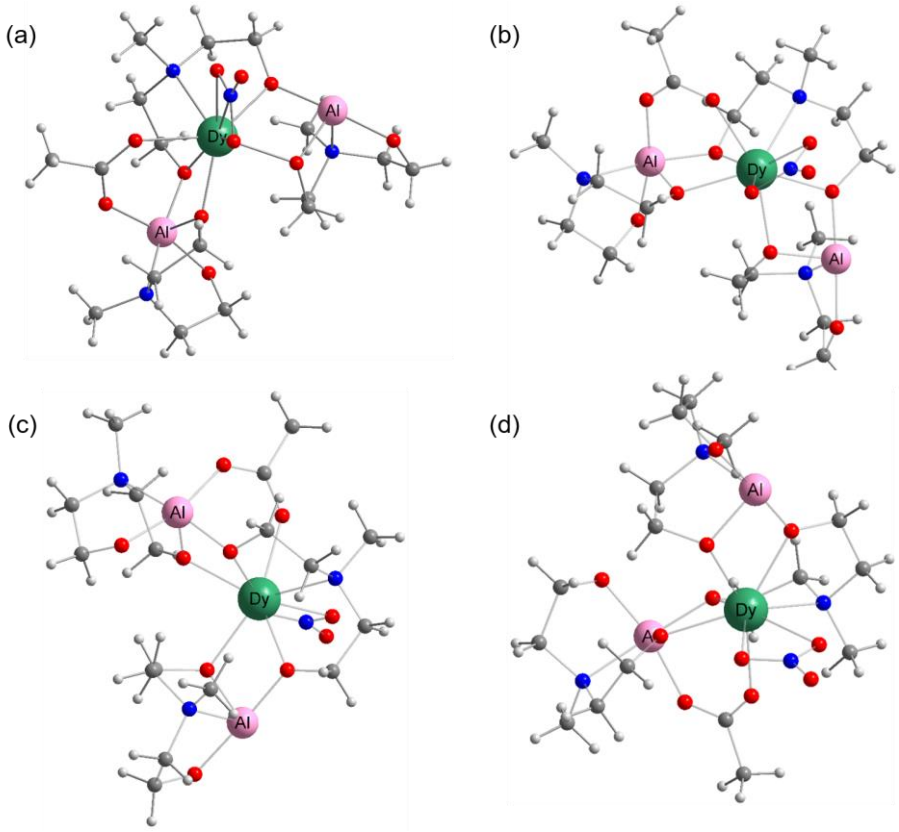

Figure S15. Calculated structure of the **2Dy-1** (a), **2Dy-2** (b), **2Dy-3** (c), and **2Dy-4** (d) fragment.

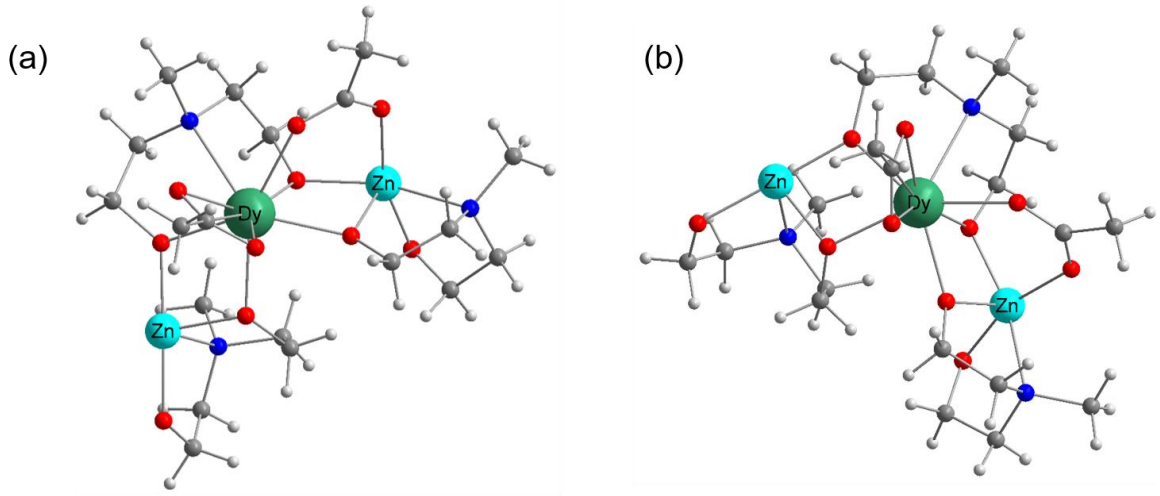

Figure S16. Calculated structure of the **1Dy-1** (a), **1Dy-2** (b) fragment.

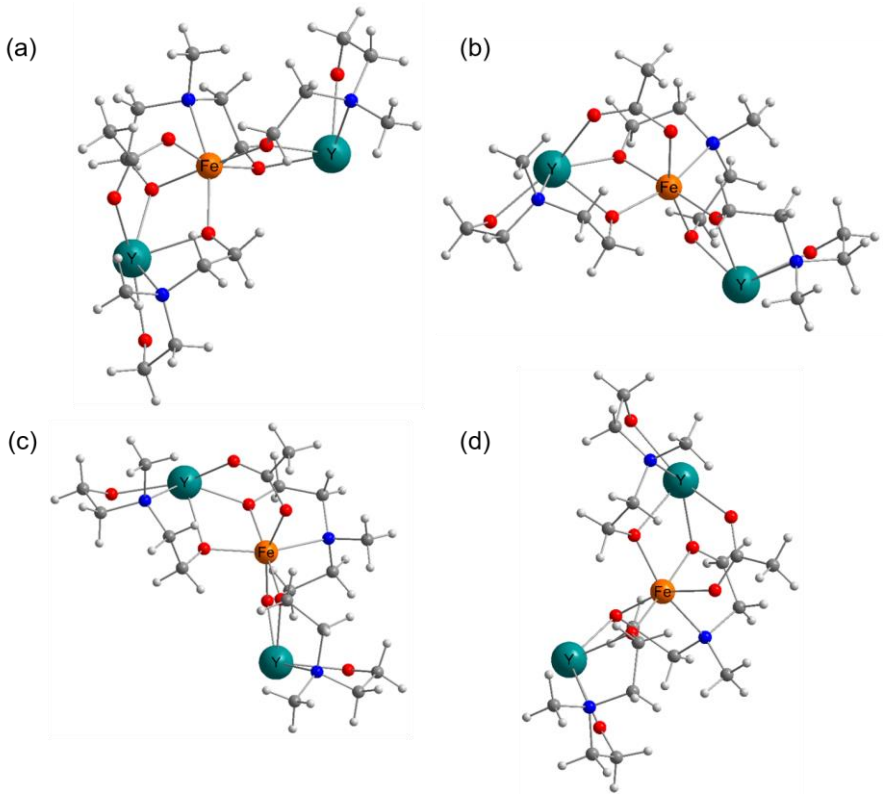

Figure S17. Calculated structure of the Fe1 (a), Fe2 (b), Fe3 (c), and Fe4 (d) fragment in **1Y.**

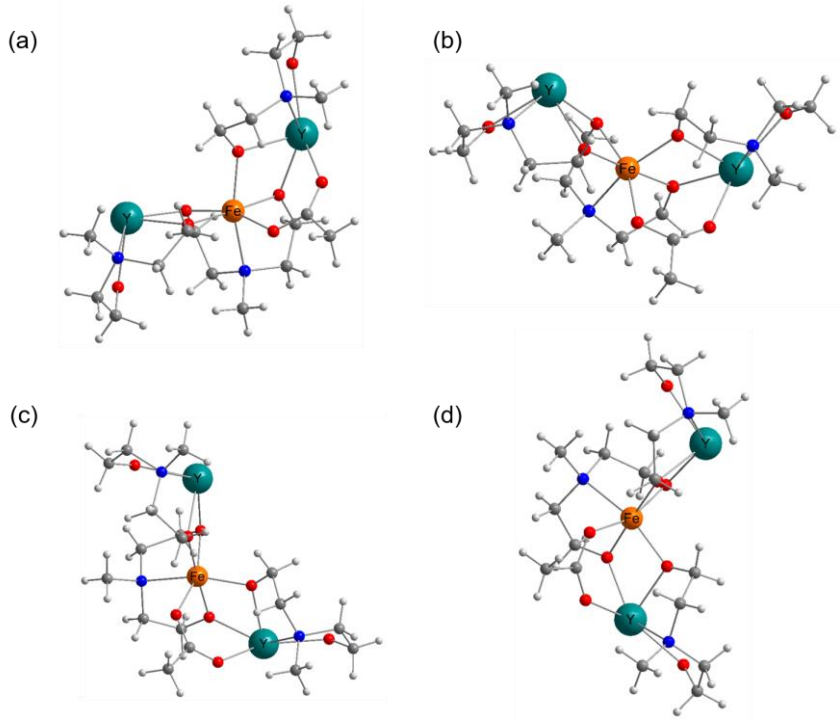

Figure S18. Calculated structure of the Fe5 (a), Fe6 (b), Fe7 (c), and Fe8 (d) fragment in **1Y.**

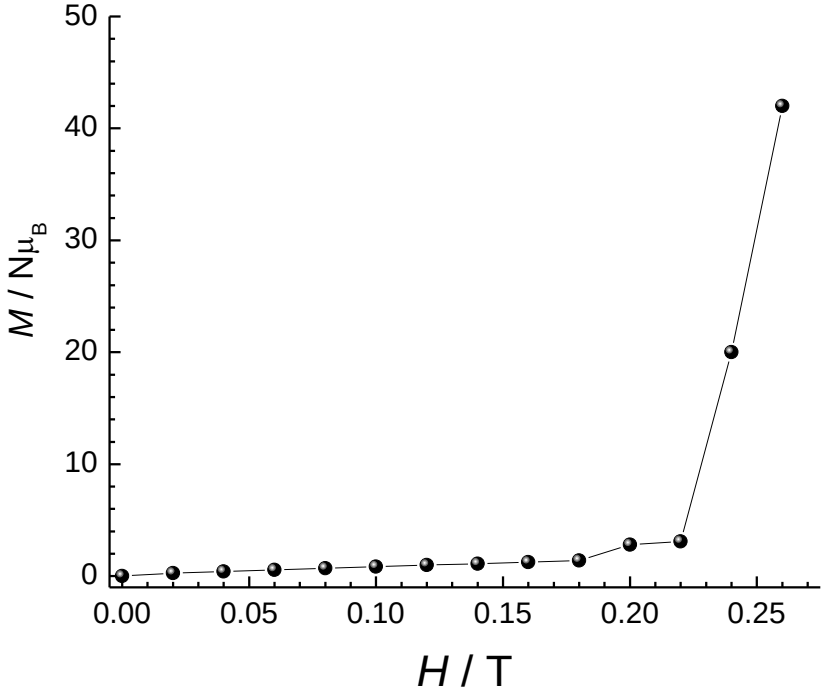

Figure S19. The simulations of field-dependent magnetization plots of **2Dy** at T ≈ 0 K.

II. Supplemental Tables

Table S1. Crystal data and structure refinement for **1Dy, 1Y** and **2Dy**.

	1Dy	**1Y**	**2Dy**
Compound	Fe_8Dy_8	Fe_8Y_8	Al_8Dy_8
Formula	$C_{114}H_{263}N_{17}Fe_8Dy_8O_{82}$	$C_{122}H_{303}N_{21}Fe_8Y_8O_{96}$	$C_{100}H_{224}N_{26}Al_8Dy_8O_{81}$
*F*w (g mol^{-1})	4931.13	4758.80	4602.82
T (K)	100(2)	100(2)	150(2)
Wavelength (Å)	0.71073	0.71073	0.71073
Crystal system	Cubic	Cubic	Orthorhombic
Space group	*Pn-3n*	*Pn-3n*	*Fddd*
a (Å)	39.853(18)	39.865(2)	20.291(11)
b (Å)	39.853(18)	39.865(2)	47.280(3)
c (Å)	39.853(18)	39.865(2)	76.050(4)
α (deg.)	90	90	90
β (deg.)	90	90	90
γ (deg.)	90	90	90
V (Å^3)	63300(5)	63358(5)	72960(70)
Z	12	12	16
D (g cm^{-3})	1.552	1.497	1.617
μ (mm^{-1})	3.405	2.793	3.359
F(000)	29496	29640	35136
Data / restraints / parameters	9322 / 26 / 476	9321 / 11 / 476	16075 / 0 / 977
Goodness-of-fit on F^2	1.175	1.092	1.177
R_1[a]	0.0874	0.1326	0.0516
wR_2 [b]	0.1896	0.2946	0.1391
CCDC Number	1942406	1942407	1942408

[a] $R_1 = \Sigma||F_o| - |F_c||/\Sigma|F_o|$, [b] $wR_2 = [\Sigma w(F_o^2-F_c^2)^2/\Sigma w(F_o^2)^2]^{1/2}$

Table S2. Selected bond lengths [Å] for **1Dy**.

Dy(1)-O(4)	2.298(8)	Dy(2)-O(14)	2.446(10)
Dy(1)-O(9)	2.310(9)	Dy(2)-N(4)	2.671(11)
Dy(1)-O(2)	2.322(8)	Fe(1)-O(3)	1.955(8)
Dy(1)-O(3)	2.331(8)	Fe(1)-O(12)#2	1.982(8)
Dy(1)-O(7)	2.395(8)	Fe(1)-O(2)	1.985(8)
Dy(1)-O(6)	2.418(9)	Fe(1)-O(1)	1.998(8)
Dy(1)-O(5)	2.433(9)	Fe(1)-O(16)#2	2.042(9)
Dy(1)-N(2)	2.661(10)	Fe(1)-N(1)	2.271(11)
Dy(2)-O(1)#1	2.298(8)	Fe(2)-O(11)	1.957(8)
Dy(2)-O(12)	2.312(8)	Fe(2)-O(10)	1.981(9)
Dy(2)-O(11)	2.318(8)	Fe(2)-O(9)	1.985(9)
Dy(2)-O(10)	2.328(8)	Fe(2)-O(4)	1.985(8)
Dy(2)-O(15)	2.381(8)	Fe(2)-O(8)	2.055(9)
Dy(2)-O(13)	2.427(8)	Fe(2)-N(3)	2.301(12)

Symmetry transformations used to generate equivalent atoms: #1 x,-z+1/2,y#2 x,z,-y+1/2

Table S3. Selected bond lengths [Å] for **2Dy**.

Al(1)-N(3)	2.127(10)	Al(4)-O(33)	1.883(8)	Dy(3)-N(7)	2.571(9)
Al(1)-O(2)	1.861(8)	Al(4)-O(34)	1.885(8)	Dy(3)-N(9)	2.878(9)
Al(1)-O(6)	1.887(7)	Al(4)-O(35)	1.908(8)	Dy(3)-O(16)	2.292(7)
Al(1)-O(7)	1.885(8)	Dy(1)-N(1)	2.596(9)	Dy(3)-O(18)	2.369(7)
Al(1)-O(8)	1.915(8)	Dy(1)-N(2)	2.862(9)	Dy(3)-O(19)	2.479(8)
Al(1)-O(13)	1.874(8)	Dy(1)-O(1)	2.296(7)	Dy(3)-O(21)	2.450(7)
Al(2)-N(5)	2.139(10)	Dy(1)-O(2)	2.328(7)	Dy(3)-O(22)	2.301(7)
Al(2)-O(14)	1.848(7)	Dy(1)-O(3)	2.435(7)	Dy(3)-O(23)	2.317(7)
Al(2)-O(15)	1.880(8)	Dy(1)-O(5)	2.472(8)	Dy(3)-O(24)	2.330(7)
Al(2)-O(16)	1.898(7)	Dy(1)-O(6)	2.320(7)	Dy(4)-N(10)	2.592(8)
Al(2)-O(17)	1.905(8)	Dy(1)-O(34)#1	2.279(7)	Dy(4)-N(11)	2.880(9)
Al(2)-O(22)	1.866(7)	Dy(1)-O(36)#1	2.371(7)	Dy(4)-O(25)	2.323(7)
Al(3)-N(8)	2.149(10)	Dy(2)-N(4)	2.591(9)	Dy(4)-O(27)	2.369(7)
Al(3)-O(23)	1.855(8)	Dy(2)-N(6)	2.865(10)	Dy(4)-O(28)	2.281(7)
Al(3)-O(24)	1.881(7)	Dy(2)-O(7)	2.293(7)	Dy(4)-O(29)	2.315(7)
Al(3)-O(25)	1.871(7)	Dy(2)-O(9)	2.357(7)	Dy(4)-O(30)	2.483(8)
Al(3)-O(26)	1.906(8)	Dy(2)-O(10)	2.435(7)	Dy(4)-O(32)	2.463(7)
Al(3)-O(28)	1.862(7)	Dy(2)-O(12)	2.481(8)	Dy(4)-O(33)	2.322(7)
Al(4)-N(12)	2.142(9)	Dy(2)-O(13)	2.299(7)	O(1)-Al(4)#1	1.868(7)
Al(4)-O(1)#1	1.868(7)	Dy(2)-O(14)	2.327(7)	O(34)-Dy(1)#1	2.279(7)
Al(4)-O(29)	1.851(8)	Dy(2)-O(15)	2.323(7)	O(36)-Dy(1)#1	2.371(7)

Symmetry transformations used to generate equivalent atoms: #1 x,-y+3/4,-z+3/4

Table S4. The *CSM* values calculated by *SHAPE* 2.1 for **1Dy** and **2Dy**.

Coordination Geometry	Atom	**1Dy**	**2Dy**
Octagon (D_{8h})		44.987	44.380
Heptagonal pyramid (C_{7v})		33.028	35.881
Hexagonal bipyramid (D_{6h})		31.189	32.254
Cube (O_h)		32.945	32.239
Square antiprism (D_{4d})		26.172	27.029
Triangular dodecahedron (D_{2d})		25.059	25.688
Johnson gyrobifastigium J26 (D_{2d})	Dy	29.763	26.693
Johnson elongated triangular bipyramid J14 (D_{3h})		41.166	39.180
Biaugmented trigonal prism J50 (C_{2v})		22.921	25.514
Biaugmented trigonal prism (C_{2v})		24.227	25.530
Snub diphenoid J84 (D_{2d})		23.246	26.450
Triakis tetrahedron (T_d)		31.386	31.536
Elongated trigonal bipyramid (D_{3h})		37.867	36.399

Table S5. The fit parameters of Cole-Cole plots for **2Dy**.

T / K	τ / s	α
3.36	4.65357×10^{-4}	0.51822
3.92	3.80131×10^{-4}	0.42390
4.34	1.73191×10^{-4}	0.06182
4.92	2.70238×10^{-4}	0.39790
5.40	2.19890×10^{-4}	0.37412
5.88	1.86709×10^{-4}	0.34987
6.37	1.63560×10^{-4}	0.32387
6.82	1.46811×10^{-4}	0.29338
7.31	1.28718×10^{-4}	0.26160
7.81	1.15114×10^{-4}	0.22864

Table S6. SA-CASSCF/RASSI calculated electronic states for **2Dy-1**.

Energy (cm^{-1})	g_x	g_y	g_z	Wavefunction
0	0.00	0.01	19.86	99.1%|±15/2>
176	0.10	0.13	16.88	94.2%|±13/2>
231	2.2	5.8	10.57	61%|±11/2> + 23%|±3/2>
288	8.6	7.2	0.50	13%|±11/2> + 17%|±1/2> + 39%|∓1/2> + 11%|∓9/2>
313	0.7	2.8	11.98	22%|±9/2> + 17%|±5/2> + 37%|∓3/2>
364	0.3	1.7	13.73	21%|±9/2> + 24%|±5/2> + 29%|∓7/2>
408	1.4	2.0	14.40	23%|±9/2> + 14%|±5/2> + 21%|±1/2> + 12%|∓3/2> + 29%|∓7/2>
436	1.3	2.5	16.49	35%|±7/2> + 21%|±3/2> + 31%|∓5/2>

[a] Only components with > 10% contribution are given, rounded to the nearest percent.

Table S7. SA-CASSCF/RASSI calculated electronic states for **2Dy-2**.

Energy (cm^{-1})	g_x	g_y	g_z	Wavefunction
0	0.00	0.01	19.46	97.1%|±15/2>
154	0.13	0.21	16.21	91.2%|±13/2>
212	1.7	7.3	9.64	43%|±11/2> + 21%|±3/2> + 10%|∓1/2>
259	7.3	6.8	3.40	11%|±9/2> + 37%|±1/2> + 24%|∓1/2>
298	1.9	3.7	10.03	12%|±9/2> + 28%|±5/2> + 32%|∓3/2>
334	0.1	0.3	16.37	49%|±9/2> + 10%|±5/2> + 34%|∓7/2>
365	3.7	5.4	13.74	20%|±11/2> + 11%|±5/2> + 21%|∓3/2> + 24%|∓7/2>
374	1.7	2.9	17.49	54%|±7/2> + 23%|±3/2> + 27%|∓5/2>

[a] Only components with > 10% contribution are given, rounded to the nearest percent.

Table S8. SA-CASSCF/RASSI calculated electronic states for **2Dy-3**.

Energy (cm^{-1})	g_x	g_y	g_z	Wavefunction
0	0.00	0.00	19.88	99.2%|±15/2>
191	0.10	0.12	16.88	94.1%|±13/2>
257	1.4	3.7	12.32	79%|±11/2> + 10%|±3/2>
307	9.3	5.9	0.24	13%|±9/2> + 17%|±1/2> + 32%|∓1/2>
347	1.4	3.7	13.13	34%|±9/2> + 27%|±7/2> + 21%|∓1/2>
378	2.5	3.7	10.13	31%|±9/2> + 24%|±5/2> + 19%|∓5/2>
418	2.7	3.4	12.43	26%|±7/2> + 10%|±5/2> + 10%|±1/2> + 13%|∓3/2>
421	3.7	5.6	11.49	31%|±7/2> + 16%|±3/2> + 29%|∓5/2>

[a] Only components with > 10% contribution are given, rounded to the nearest percent.

Table S9. SA-CASSCF/RASSI calculated electronic states for **2Dy-4**.

Energy (cm^{-1})	g_x	g_y	g_z	Wavefunction
0	0.00	0.01	19.87	99.2%|±15/2>
167	0.10	0.13	16.86	94.3%|±13/2>
224	2.7	5.9	11.03	62%|±11/2> + 24%|±3/2>
279	5.6	4.2	3.05	11%|±11/2> + 37%|±1/2> + 14%|∓7/2>
301	0.7	6.3	10.58	25%|±9/2> + 49%|∓3/2>
347	1.2	3.8	14.39	22%|±9/2> + 29%|±5/2> + 31%|∓7/2>
389	2.4	4.0	16.41	21%|±7/2> + 14%|±3/2> + 10%|∓3/2> + 19%|∓5/2>
403	2.9	5.5	13.27	31%|±7/2> + 21%|±3/2>

[a] Only components with > 10% contribution are given, rounded to the nearest percent.

Table S10. The individual deviation angles from the plane and corresponding Ising interactions of **2Dy**. (in cm^{-1})

	$cos\varphi$	$\widetilde{J_\iota}$
2Dy-1 with 2Dy-2	-0.10009	0.02502
2Dy-2 with 2Dy-3	-0.06993	0.01748
2Dy-3 with 2Dy-4	-0.12242	0.0306
2Dy-4 with 2Dy-1'	-0.04336	0.01084
…		

Table S11. The angle (θ) of anisotropy axis tilting with Dy_8 plane in **2Dy**.

Anisotropy axis	θ / ∘
2Dy-1	44.55
2Dy-2	42.01
2Dy-3	42.64
2Dy-4	42.01
2Dy-1'	44.55
2Dy-2'	42.01
2Dy-3'	42.64
2Dy-4'	42.01

Table S12. The calculated *g* tensors for the lowest and four different kinds of first excited Kramers doublets of **2Dy**.

	|0>	|1-1>	|1-2>	|1-3>	|1-4>
g_y	0.00	0.00	0.01	0.01	0.03
g_z	0.00	0.01	0.01	0.04	0.07
g_x	0.42	39.37	38.14	38.32	37.10

Table S13. The magnetic parameters of **1Y** extracted from *ab initio* calculations.

	D (cm^{-1})	E/D	g_x	g_y	g_z
Fe1	-0.32	0.20	1.99	1.99	1.99
Fe2	-0.14	0.20	1.99	1.99	1.99
Fe3	-0.31	0.21	1.99	1.99	1.99
Fe4	-0.17	0.20	1.99	1.99	1.99
Fe5	-0.29	0.21	1.99	1.99	1.99
Fe6	-0.15	0.21	1.99	1.99	1.99
Fe7	-0.31	0.17	1.99	1.99	1.99
Fe8	-0.14	0.20	1.99	1.99	1.99

Table S14. SA-CASSCF/RASSI calculated electronic states for **1Dy-1**.

Energy (cm^{-1})	g_x	g_y	g_z	Wavefunction
0	0.43	1.21	18.16	70%|±15/2> + 23%|±13/2>
81	3.41	4.27	10.94	54%|±13/2> + 10%|±11/2> + 24%|±1/2>
154	0.9	4.9	9.87	41%|±11/2> + 13%|±9/2> + 25%|∓3/2>
203	8.1	5.1	4.21	10%|±13/2> + 12%|±11/2> + 58%|∓5/2>
231	1.2	3.4	13.73	12%|±15/2> + 21%|±7/2> + 57%|∓3/2>
304	3.1	4.5	8.67	31%|±9/2> + 24%|±7/2> + 17%|∓5/2>
378	0.9	1.2	16.32	25%|±13/2> + 10%|±3/2> + 23%|±1/2> + 29%|∓7/2>
405	1.7	3.4	13.27	35%|±7/2> + 31%|±3/2> + 10%|∓5/2> + 11%|±1/2> + 10%|∓7/2>

[a] Only components with > 10% contribution are given, rounded to the nearest percent.

Table S15. SA-CASSCF/RASSI calculated electronic states for **1Dy-2**.

Energy (cm^{-1})	g_x	g_y	g_z	Wavefunction
0	0.58	1.71	17.69	67%|±15/2> + 19%|±13/2> + 10%|±1/2>
62	2.74	3.98	12.74	63%|±13/2> + 34%|±1/2>
117	0.5	2.9	14.35	61%|±11/2> + 23%|±7/2> + 10%|∓3/2>
145	8.4	4.3	2.92	50%|±9/2> + 32%|±7/2>
169	0.3	1.9	16.14	14%|±15/2> + 41%|±9/2> + 17%|∓1/2>
214	4.3	6.9	7.84	34%|±7/2> + 37%|∓5/2>
269	3.1	4.9	11.12	40%|±3/2> + 13%|±1/2> + 19%|∓7/2>
324	1.2	2.7	15.41	29%|±3/2> + 37%|∓5/2> + 23%|±1/2> + 10%|∓11/2>

[a] Only components with > 10% contribution are given, rounded to the nearest percent.